Polyhedron 67 (2014) 495–504

Contents lists available at ScienceDirect

Polyhedron

journal homepage: www.elsevier.com/locate/poly

Bis(μ-alkoxo) bridged dinuclear Cu^{II}_2 and Zn^{II}_2 complexes of an isoindol functionality based new ligand: Synthesis, structure, spectral characterization, magnetic properties and catechol oxidase activity

Ayan Patra [a], Gopal C. Giri [a], Tamal K. Sen [b], Luca Carrella [c], Swadhin K. Mandal [b], Manindranath Bera [a,*]

[a] Department of Chemistry, University of Kalyani, Kalyani 741235, West Bengal, India
[b] Department of Chemical Sciences, Indian Institute of Science Education & Research Kolkata, Mohanpur 741252, West Bengal, India
[c] Institut fur Anorganische Chemie und Analytische Chemie, Johannes-Gutenberg, Universitat Mainz, Duesbergweg 10-14, D-55128 Mainz, Germany

ARTICLE INFO

Article history:
Received 5 July 2013
Accepted 29 September 2013
Available online 14 October 2013

Keywords:
Dinucleating ligand
Isoindol functionality
Copper(II)/zinc(II)
Magnetism
Catecholase activity
DFT calculations

ABSTRACT

Two new dinuclear copper(II) and zinc(II) complexes of an isoindol functionality based new dinucleating ligand, H_3hdpa (H_3hdpa = 2-({[2-hydoxyethyl]-[2-hydroxy-3-(1-oxo-1,3-dihydro-isoindol-2-yl)-propyl]-amino}-methyl)-benzoic acid) have been synthesized and characterized. In methanol, the reaction of stoichiometric amounts of $Cu(OAc)_2{\cdot}H_2O$ and the ligand H_3hdpa in the presence of NaOH at ambient temperature afforded a new dinuclear copper(II) complex, $[Cu_2(Hhdpa)_2]{\cdot}2CH_3OH{\cdot}6H_2O$ (**1**). Similarly, in methanol, the reaction of stoichiometric amounts of $Zn(OAc)_2{\cdot}2H_2O$ and H_3hdpa in the presence of NaOH yielded a new dinuclear zinc(II) complex, $Na_4[Zn_2(hdpa)_2](OAc)_2$ (**2**). Characterization of the complexes has been performed using various analytical techniques, including single crystal X-ray structure determination. The X-ray crystal structure of complex **1** reveals that two copper(II) centers adopt a five-coordinate square pyramidal geometry with a Cu–Cu separation of 2.910 Å. The DFT optimized structure of complex **2** shows that two zinc(II) centers are in a distorted trigonal bipyramidal geometry with a Zn–Zn separation of 3.124 Å. ^{1}H and ^{13}C NMR spectroscopic investigations authenticate the integrity of complex **2** in solution. Further, the mass spectroscopic analyses of complexes **1** and **2** reconfirm their dimeric nature, even in solution. Variable-temperature (2–300 K) magnetic susceptibility measurements show the presence of antiferromagnetic interactions ($J = -52.20$ cm^{-1}) between the two copper(II) centers in complex **1**. The catechol oxidase activity of complexes **1** and **2** has been investigated in methanol medium by the UV–Vis spectrophotometric technique using 3,5-di-tert-butylcatechol as a model substrate. Both complexes are active in catalyzing the aerobic oxidation of 3,5-di-tert-butylcatechol (3,5-DTBC) to 3,5-di-tert-butyl-1,2-benzoquinone (3,5-DTBQ). A DFT calculation has been performed to find the Fukui functions at the metal centers in complexes **1** and **2** to predict the possible metal centers involved in the binding process with 3,5-DTBC during the catalytic oxidation reactions.

1. Introduction

Dimetallic complexes have been recognized at the active sites of many metalloenzymes [1]. In fact, enzyme models are of practical importance for the development of efficient molecular catalysts for organic reactions and of theoretical importance in elucidating the mechanisms of enzymatic reactions [2]. So, model studies with simple dinuclear metal complexes are becoming increasingly important in understanding the biological functions of dimetallic cores [3]. Very often, in a dimetallic system, one metal ion is responsible for substrate binding while the other delivers the activated solvent nucleophile for hydrolysis. Dinuclear Cu_2 and Zn_2 complexes, with either one loosely bound apical exogeneous ligand or coordinatively unsaturated ligand, have the potential for binding biologically important substrates, thereby providing new reactivity patterns. In this context, dinuclear copper(II) complexes with two metal ions in close proximity have received considerable attention as structural models for catechol oxidase (CO), which catalyzes the oxidation of o-diphenol to o-quinone coupled with a $2e^-/2H^+$ reduction of O_2 to H_2O [4]. The crystal structures of CO isolated from sweet potato [5] reveals that the active site of the enzyme contains antiferromagnetically coupled EPR silent Cu_2 centers in which the Cu–Cu distance is 2.9 Å, which is a suitable distance for catechol binding [6]. In isolated CO, each copper(II) center is coordinated to three histidine nitrogen atoms and is bridged by an external hydroxo group in a trigonal pyramidal geometry. Thus, oxygen bridged dinuclear copper(II) complexes have attracted great attention in recent years. As a result, a number of dinuclear copper(II) complexes are well documented in the

* Corresponding author. Tel.: +91 33 25828282x306; fax: +91 33 25828282.
E-mail address: mbera2009@klyuniv.ac.in (M. Bera).

0277-5387/$ - see front matter © 2013 Elsevier Ltd. All rights reserved.
http://dx.doi.org/10.1016/j.poly.2013.09.034

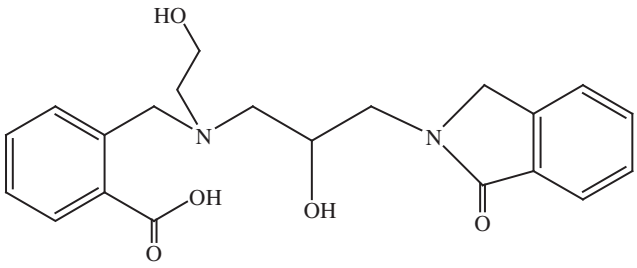

Fig. 1. Chemical structure of the ligand 2-({[2-hydoxyethyl]-[2-hydroxy-3-(1-oxo-1,3-dihydro-isoindol-2-yl)-propyl]-amino}-methyl)-benzoic acid, H_3hdpa.

literature for understanding the mode of catechol binding and the mechanistic role of the active site [7]. In contrast, dinuclear zinc(II) complexes remain largely unexplored as synthetic models for catechol oxidase activity [8]. However, a few interesting reports on the interactions of zinc complexes with model substrates like 3,5-di-tert-butylcatechol (3,5-DTBC) or tetrachlorocatechol(TCC) are reported in the literature [9].

Recently, the coordination behaviors of various dinucleating ligands containing alkoxo and carboxylato donor groups have been reported in the literature [10]. The use of dinucleating carboxylate ligands as organic linkers which are capable of binding two metal ions through direct bond formation and promoting magnetic interactions has been studied extensively [11]. We have focused here on an isoindol ring containing new dinucleating ligand, H_3hdpa (Fig. 1). During N-alkylation of one half of the symmetrical precursor ligand, *N,N′*-bis(2-carboxybenzomethyl)-1,3-diaminopropan-2-ol (H_3cdp) [12] with 2-iodoethanol in a 1:1 M ratio, the secondary amine and the benzoate functionality of the other half of the ligand undergo an intramolecular cyclization reaction to produce a new unsymmetrical ligand, H_3hdpa, consisting of an isoindol functionality. The 1-oxo-1,3-dihydroisoindol ring is most likely achieved via a known mechanism that involves the activation of the secondary amine and benozoate backbone in the presence of NaOH [13]. In this paper, we report the synthesis, structure, spectroscopic characterization, magnetic properties and catechol oxidase activity of a new dinuclear copper(II) and a new dinuclear zinc(II) complex.

2. Experimental

2.1. Materials

2-Carboxybenzaldehyde, 1,3-diamino-2-propanol, 2-iodoethanol and 3,5-di-tert-butyl catechol were purchased from Sigma–Aldrich Chemie GmbH, Germany. Zinc acetate dihydrate and copper acetate monohydrate were purchased from Merck, India. All other chemicals and solvents were reagent grade materials and were used as received from commercial sources without further purification.

2.2. Physical measurements

Microanalyses (C,H,N) were performed using a Perkin–Elmer 2400 CHNS/O Series II elemental analyzer. FTIR spectra were obtained on a Perkin–Elmer L120-000A spectrometer (200–4000 cm^{-1}). ^1H and ^{13}C NMR spectra were obtained in D_2O and DMSO-d^6 solutions on a Bruker AC 400 NMR spectrometer using TMS as the internal standard. Mass spectra were recorded in a MALDI-TOF MS using a Perseptive Bio System Voyager DE-STR mass spectrometer. UV–Vis spectra were recorded on a Shimadzu UV 1800 (190–1100 nm) (1 cm quartz cell) spectrophotometer. The room temperature magnetic susceptibilities in the solid state were measured using a home built Gouy balance fitted with a polytronic d.c. power supply. The variable temperature magnetic susceptibility data for complex **1** was collected in a temperature range of 2–300 K under an applied field of 1 Tesla on a powdered microcrystalline sample with a SQUID magnetometer (MPMS-7, Quantum Design). Experimental susceptibility data were corrected for the underlying diamagnetism using Pascal's constants [14]. The temperature dependent magnetic contribution of the holder was experimentally determined and subtracted from the measured susceptibility data. The program julx was used for spin Hamiltonian simulations of the data [15].

2.3. Synthesis of 2-({(2-hydroxy-ethyl)-[2-hydroxy-3-(1-oxo-1,3-dihydro-isoindol-2-yl)-propyl]-amino}-methyl)-benzoic acid, H_3hdpa

A solution of 2-carboxybenzaldehyde (4.643 g, 30.00 mmol) and NaOH (1.200 g, 30.00 mmol) in 100 ml methanol was added to 1,3-diamino-propan-2-ol (1.424 g, 15.00 mmol) in 20 ml methanol. The yellowish mixture obtained was heated to 60 °C while stirring for ~ 4 h. The reaction product then was cooled in an ice-bath. Excess $NaBH_4$ (1.500 g, 39.50 mmol) was added in portions to the cold solution while stirring. The yellow color was slightly discharged. After 30 min, 2 ml conc. HCl (12 M) was added dropwise to destroy the excess $NaBH_4$. Acidification of the solution to pH ~ 5 by addition of more HCl resulted in the precipitation of a crystalline white solid. The white solid was filtered out from the mother liquor and washed with H_2O and methanol, and dried at ~80 °C. Yield: 4.95 g (87%). The compound crystallizes with one molecule of water, as found from the elemental analysis, and was characterized as $H_3cdp{\cdot}H_2O$. *Anal.* Calc. for $C_{19}H_{22}N_2O_5{\cdot}H_2O$: C, 60.63; H, 6.43; N, 7.44. Found: C, 60.25; H, 6.28; N, 7.33%. ^1H NMR for the sodium salt of the compound (400 MHz, D_2O, 25 °C, δ (ppm)): 7.46–7.32 (m, 8H), 3.92–3.80 (m, 1H), 2.63 (q, 4H), 2.55 (q, 4H).

A solution of 2-iodoethanol (0.859 g, 5.00 mmol) was added dropwise to a solution of *N,N′*-bis(2-carboxybenzomethyl)-1,3-diaminopropan-2-ol (H_3cdp) (1.790 g, 5.00 mmol) and NaOH (0.400 g, 10.00 mmol) in 25 ml of water and the whole reaction mixture was refluxed for ~4 h. While refluxing, more NaOH (0.200 g, 5.00 mmol) was added in portions to maintain the pH of the solution at ~12. The resulting solution was cooled and acidified with conc. HCl (12 M) to pH ~5. The solution was then rotary evaporated under vacuum to isolate an off white solid product which was washed with acetone and hexane. The product was confirmed by elemental analysis, FTIR, ^1H and ^{13}C NMR and mass spectroscopy. *Anal.* Calc. for $C_{21}H_{24}N_2O_5$: C, 65.61; H, 6.29; N, 7.29. Found: C, 65.44; H, 6.36; N, 7.16%. FTIR (ν, cm^{-1}): 3413(b), 2955(b), 1661(s), 1588(vs), 1564(s), 1456(s), 1399(s), 1213(s), 1153(s), 1091(s), 871(s), 740(s). ^1H NMR for the sodium salt of the compound (400 MHz, D_2O, room temperature, δ (ppm)): 7.65 (d, 1H), 7.53 (d, 1H), 7.48 (d, 1H), 7.44 (d, 1H), 7.40 (d, 1H), 7.21 (m, 1H), 7.13 (t, 1H), 6.88 (t, 1H), 4.55 (t, 2H), 4.19–4.30 (m, 1H), 3.98 (s, 2H), 3.64 (d, 2H), 3.50 (d, 2H), 3.28 (s, 2H), 2.87 (t, 2H). ^{13}C NMR (400 MHz, D_2O, room temperature, δ (ppm)): 179.07, 171.57, 140.48, 134.72, 131.94, 130.90, 128.68, 128.36, 127.71, 126.70, 123.60, 123.09, 66.35, 62.92, 59.09, 58.45, 57.13, 46.09, 49.54. Mass spectrum (ESI) m/z: 407 (M^+ = {H_3hdpa + Na}$^+$).

2.4. Synthesis of $[Cu_2(Hhdpa)_2]{\cdot}2CH_3OH{\cdot}6H_2O$ (**1**)

A methanol solution (10 ml) of $Cu(OAc)_2{\cdot}H_2O$ (0.130 g, 0.65 mmol) was slowly added to a magnetically stirred methanol solution (15 ml) of the ligand H_3hdpa (0.250 g, 0.65 mmol) and NaOH (0.078 g, 1.95 mmol) at ambient temperature over a period of 15 min. The reaction mixture was stirred for 1 h, resulting in a green solution. It was then filtered to discard any insoluble precipitates. X-ray quality bluish-green block shaped single crystals were obtained by a slow ether diffusion into the clear filtrate after

~7 days. Yield: 0.220 g (76%). *Anal.* Calc. for $C_{42}H_{44}Cu_2N_4O_{10}$: C, 56.56; H, 4.97; N, 6.28; Cu, 14.25. Found: C, 56.85; H, 4.81; N, 6.34; Cu, 14.19%. FTIR (KBr, ν, cm^{-1}): 3400(b), 1656(s), 1587(s), 1474(s), 1382(s), 1211(s), 1102(s), 1087(s), 958(s), 898(s), 809(s), 740(s). UV–Vis (MeOH) λ_{max} (ε, L mol^{-1} cm^{-1}): 728 (181), 292 (1355)^{sh}, 221 (31434). Mass spectrum (ESI) m/z: 914 (M^+ = {[Cu_2(-Hhdpa)$_2$]+Na}$^+$). μ_{eff} (tot.): 2.42 μ_B; μ_{eff}/Cu: 1.71 μ_B.

2.5. Synthesis of $Na_4[Zn_2(hdpa)_2](OAc)_2$ (2)

A methanol solution (10 ml) of $Zn(OAc)_2{\cdot}2H_2O$ (0.143 g, 0.65 mmol) was slowly added to a magnetically stirred methanol solution (15 ml) of the ligand H_3hdpa (0.250 g, 0.65 mmol) and NaOH (0.078 g, 1.95 mmol) at ambient temperature over a period of 10 min. The reaction was stirred at room temperature for 2 h. It was then filtered to discard any insoluble precipitates. The clear filtrate was then rotary evaporated under vacuum to obtain a colorless solid product which was washed thoroughly with acetone and water. The product was dried and finally confirmed by elemental analysis, FTIR, ^{1}H and ^{13}C NMR and mass spectroscopy. Yield: 0.233 g (65%). *Anal.* Calc. for $C_{46}H_{48}N_4O_{14}Na_4Zn_2$: C, 50.06; H, 4.38; N, 5.08; Zn, 11.85. Found: C, 50.39; H, 4.45; N, 5.19; Zn, 12.16%. FTIR (KBr, ν, cm^{-1}): 3437(b), 1656(s), 1591(s), 1567(s), 1399(s), 1340(s), 1213(s), 1154(s), 1022(s), 933(s), 866(s), 758(s), 738(s), 673(s). ^{1}H NMR (DMSO-d^6, δ (ppm)): 1.80 (s, 6H, methyl), 2.88 (s, 4H, methylenic), 3.47–4.71 (m, 18H, ethylenic), 4.59 (s, 4H), 7.48–7.94 (m, 16H, aromatic). ^{13}C NMR (DMSO-d^6, δ (ppm)): 23.17 (2C, CH_3), 30.84 (2C, CH_2), 35.88 (2C, CH_2), 46.39 (4C, CH_2), 51.12 (2C, CH_2), 62.79 (2C, CH_2), 68.10 (2C, CH), 122.71 (2C, aromatic CH), 123.33 (2C, aromatic CH), 127.67 (2C, aromatic CH), 127.78 (2C, aromatic CH), 127.92 (2C, aromatic CH), 128.45 (2C, aromatic CH), 129.15 (2C, aromatic CH), 131.28 (2C, aromatic CH), 132.00 (2C, aromatic CH), 132.32 (2C, aromatic CH), 132.43 (2C, aromatic CH), 142.25 (2C, aromatic CH), 162.40 (2C, isoindol carbonyl group), 167.68 (2C, aliphatic carboxylate), 177.17 (2C, aromatic carboxylate). Mass spectrum (ESI) m/z: 1014 (M^- = {[Zn_2(hdpa)$_2$](OAc)$_2$+3H}$^-$).

Table 1
Crystal data and structure refinement for **c**omplex **1**.

Empirical formula	$C_{44}H_{64}Cu_2N_4O_{18}$
Formula weight	1064.09
Crystal system	monoclinic
Space group	*P*2/*c*
a (Å)	22.313(2)
b (Å)	11.6376(11)
c (Å)	18.5397(17)
α (°)	90.00
β (°)	92.194(2)
γ (°)	90.00
V	4810.7(8)
Z	4
D_{calc} (Mg/m^3)	1.469
Wavelength (Å)	0.71073
T (K)	100
F(000)	2232
Absorption coefficient (mm^{-1})	0.962
θ (°)	1.75–28.48
Reflections collected	12013
Independent reflections	9902
R(*F* obsd data) [$I > 2\sigma(I)$]	0.0359
wR(F^2 all data)	0.0920
Goodness-of-fit (GOF) on F^2	1.041
Largest difference in peak and hole (e/Å^3)	+0.796 and −0.944

$wR_2 = \{\sum[w(F_o^2 - F_c^2)^2]/\sum[w(F_o^2)^2]\}1/2$.
$R1 = \sum||F_o| - |F_c||/\sum|F_o|$.

2.6. X-ray diffraction study

Crystal data and refinement parameters for complex **1** are summarized in Table 1. Selected bond distances and bond angles are given in Table 2. A clear bluish-green block shaped single crystal of complex **1** with approximate dimensions of 0.197 × 0.156 × 0.113 mm was selected for structural analysis. The intensity data for this compound were collected using a diffractometer with a Bruker SMART CCD area detector [16] and graphite-monochromated Mo Kα radiation (λ = 0.71073 Å). The monoclinic space group *P*2/*c* was determined by statistical tests and verified by subsequent refinement. Data were collected at 100 K. For complex **1**, a total of 12013 data were measured with Miller indices h_{min} = −29, h_{max} = 29, k_{min} = −15, k_{max} = 14, l_{min} = −24, l_{max} = 24, in the range 1.75 < θ < 28.48° using ω oscillation frames. The data were corrected for absorption by the multi-scan method [17] giving minimum and maximum transmission factors. The data were merged to form a set of 9902 independent reflections with R = 0.0359. The structure was solved by direct methods and refined by full-matrix least-squares methods on F^2 [18]. The hydrogen atom positions were initially determined by geometry and refined by a riding model. Non-hydrogen atoms were refined with anisotropic displacement parameters. All hydrogen atoms were generated in ideal positions (C–H, 0.96 Å), and fixed with isotropic thermal parameters. Actually, the structure contains two methanol molecules, with one disordered over two positions, and six water molecules which are connected together *via* hydrogen bridges.

2.7. Catechol oxidase activity studies

In order to study the catecholase activity of the complexes, solutions of **1** and **2** in unbuffered methanol solution (0.5×10^{-4} M) were treated separately with 100 equivalents of 3,5-di-tert-butylcatechol (3,5-DTBC) under aerobic conditions at room temperature. Absorbance *vs* wavelength plots were recorded for these solutions at a regular time interval of 5 min in the range 300–500 nm. The dependence of rate on the substrate concentration and various kinetic parameters were determined by treating a 0.5×10^{-4} M solution of complexes **1** and **2** with different concentrations of 3,5-DTBC to maintain the pseudo first order reaction conditions. The reactions were followed spectrophotometrically by monitoring the increase in the absorbance band of 3,5-di-tert-butyl-1,2-benzoquinone (3,5-DTBQ) at 400 nm (ε = 1900 M^{-1} cm^{-1}) as a function of time.

Table 2
Selected bond lengths (Å) and angles (deg) in complex **1**.

Bond lengths (Å)	
Cu(1)–O(2)	1.9300(13)
Cu(1)–O(2*)	1.9471(13)
Cu(1)–O(4)	1.9549(13)
Cu(1)–N(2)	2.0239(16)
Cu(1)–O(3)	2.2884(14)
Bond angles (°)	
O(2)–Cu(1)–O(2*)	78.85(6)
O(2*)–Cu(1)–O(4)	162.00(6)
O(2)–Cu(1)–O(4)	99.32(6)
O(2*)–Cu(1)–N(2)	85.39(6)
O(2)–Cu(1)–N(2)	163.79(6)
O(4)–Cu(1)–N(2)	96.84(6)
O(2*)–Cu(1)–O(3)	111.92(6)
O(2)–Cu(1)–O(3)	99.44(5)
O(4)–Cu(1)–O(3)	86.07(6)
N(2)–Cu(1)–O(3)	82.83(6)

Symmetry code: '−*x*, *y*, −*z* + 1/2'.
* To indicate the equivalent oxygen atoms.

2.8. DFT calculations

DFT calculations regarding the structure optimization of complex **2** and the Fukui functions (f_k^+) of the metal sites of complexes **1** and **2** were carried out with the Gaussian 03 software [19]. The functions (f_k^+) were evaluated from single point calculations using the UB3LYP and B3LYP methods [20] and the LanL2DZ [21] basis set at the optimized geometry, performed for N and $(N+1)$ electron systems, where N is the total number of electrons in the system. In a finite difference approximation, f_k^+ of atom k, in molecule with N electrons, is expressed by the equation $f_k^+ = [q_k(N) - q_k(N+1)]$, where q_k is the charge of atom k [22]. The q_k values were calculated by Mulliken population analysis (MPA).

3. Results and discussion

3.1. Syntheses and characterizations

The unsymmetrical dinucleating ligand H_3hdpa has been synthesized in a two step reaction as shown in Scheme 1. The synthesis of the precursor reduced Schiff base, H_3cdp, has been accomplished by the condensation of stoichiometric amounts of 2-carboxybenzaldehyde and 1,3-diamino-propan-2-ol in the presence of NaOH in methanol under refluxing conditions for 4 h, followed by the subsequent reduction using $NaBH_4$ [12]. Acidification of the resulting solution by addition of HCl to pH ~ 5 yielded a white solid product. The product has been characterized to be the reduced Schiff base H_3cdp·H_2O by different analytical techniques, such as elemental analysis, FTIR and NMR spectroscopy. Alkylation of the secondary amine of one half of H_3cdp with 2-iodoethanol in a 1:1 M ratio and intramolecular cyclization between the secondary amine and the benzoate functionality of the other half produced the dinucleating ligand H_3hdpa in good yield. The ligand H_3hdpa was fully characterized using elemental analysis, FTIR, NMR (Figs. S1 and S2 in the SI) and mass (Fig. S3 in the SI) spectroscopic techniques.

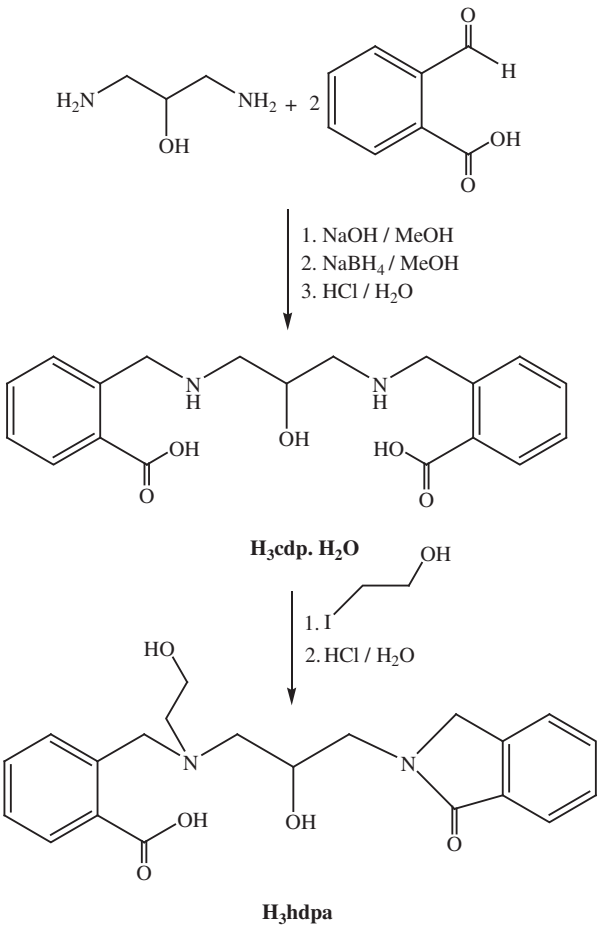

Scheme 1. Synthesis of the ligand H_3hdpa.

The reaction of $Cu(OAc)_2{\cdot}H_2O$ with the ligand H_3hdpa in a 1:1 M ratio in the presence of a strong base, NaOH, at pH ~ 9 in methanol afforded a green dinuclear complex, $[Cu_2(Hhdpa)_2]{\cdot}2CH_3OH{\cdot}6H_2O$ (**1**) (Scheme 2). However, the reaction of $Zn(OAc)_2{\cdot}2H_2O$ with H_3hdpa in a 1:1 M ratio in the presence of NaOH at pH ~ 9 in methanol yielded an off-white dinuclear complex, $Na_4[Zn_2(hdpa)_2](OAc)_2$ (**2**) (Scheme 2). Complexes **1** and **2** were fully characterized using techniques such as elemental analysis, FTIR, UV–Vis, ^{1}H and ^{13}C NMR spectral analyses and room temperature magnetic moment measurements. The room temperature magnetic moment per Cu for complex **1** is 1.71 μ_B, indicating the presence of one unpaired electron for each copper ion.

3.2. Description of the X-ray crystal structure of $[Cu_2(Hhdpa)_2]{\cdot}2CH_3OH{\cdot}6H_2O$ (**1**)

The single crystal X-ray structure of complex **1** contains two half molecules in the asymmetric unit and the dinuclear complex is formed through a twofold axis in the space group $P2/c$ with equivalent structures of the formula $[Cu_2(Hhdpa)_2]{\cdot}2CH_3OH{\cdot}6H_2O$. Each independent dinuclear species then displays crystallographic $C2$ symmetry with the 2-fold axis passing through the $[Cu_2O_2]$ ring of each dimer. A structural view of one of these dinuclear copper(II) molecules is depicted in Fig. 2. The cystal structure of each dimer of complex **1** consists of a neutral species, $[Cu_2(Hhdpa)_2]$, along with two methanol and six water molecules of crystallization. In the neutral species $[Cu_2(Hhdpa)_2]$, two equivalent copper(II) ions are bridged by the central alkoxo oxygen atoms of the two ligands, forming a $Cu_2(OR)_2$ central core. Both copper(II) ions adopt a five-coordinate distorted square pyramidal geometry, each provided by the two bridging alkoxo oxygens, one terminal alcohol oxygen, one tertiary amine nitrogen and one benzoate oxygen atom of the ligand. The square pyramidal geometry around each copper center is defined by the O(2), O(2*), O(4) and N(2) atoms at the equatorial position and O(3) at the axial position. The deviations of the four donor atoms O(2), O(2*), O(4) and N(2) describing the basal plane of Cu(1) from the least-squares mean plane through them are 0.170, 0.187, 0.138 and 0.155 Å, respectively. The Cu(1) atom is displaced by 0.168 Å from the same plane towards the axially coordinated O(3) atom. The equatorial bond lengths around the Cu(1) atom are in the range 1.9300(13)–2.0239(16) Å. The Cu(1)–O(3) axial bond distance is significantly longer than the other equatorial bond distances [2.2884(14) versus 2.0239(16) Å]. The longer Cu(1)–O(3) axial bond distance is in agreement with the reported values in the literature [23,24]. The Cu–Cu separation in the dinuclear unit is 2.9109(5) Å, which is consistent with values reported in the literature [25,26]. More interestingly, the solid state X-ray crystal structure of complex **1** shows that the isoindol functionality at the half end of the ligand $hdpa^{3-}$ remains uncoordinated to any of the copper(II) centers. Two coordinated benzoate and two uncoordinated isoindol functionalities are significantly tilted in the same direction from the Cu(1)–O(2)–Cu(1*)–O(2*) plane.

3.3. DFT optimized structure of $Na_4[Zn_2(hdpa)_2](OAc)_2$ (**2**)

Since we failed in our attempts to isolate single crystals of complex **2** suitable for X-ray diffraction analysis, the structure of **2** was optimized by DFT methods. Full optimization was carried out for

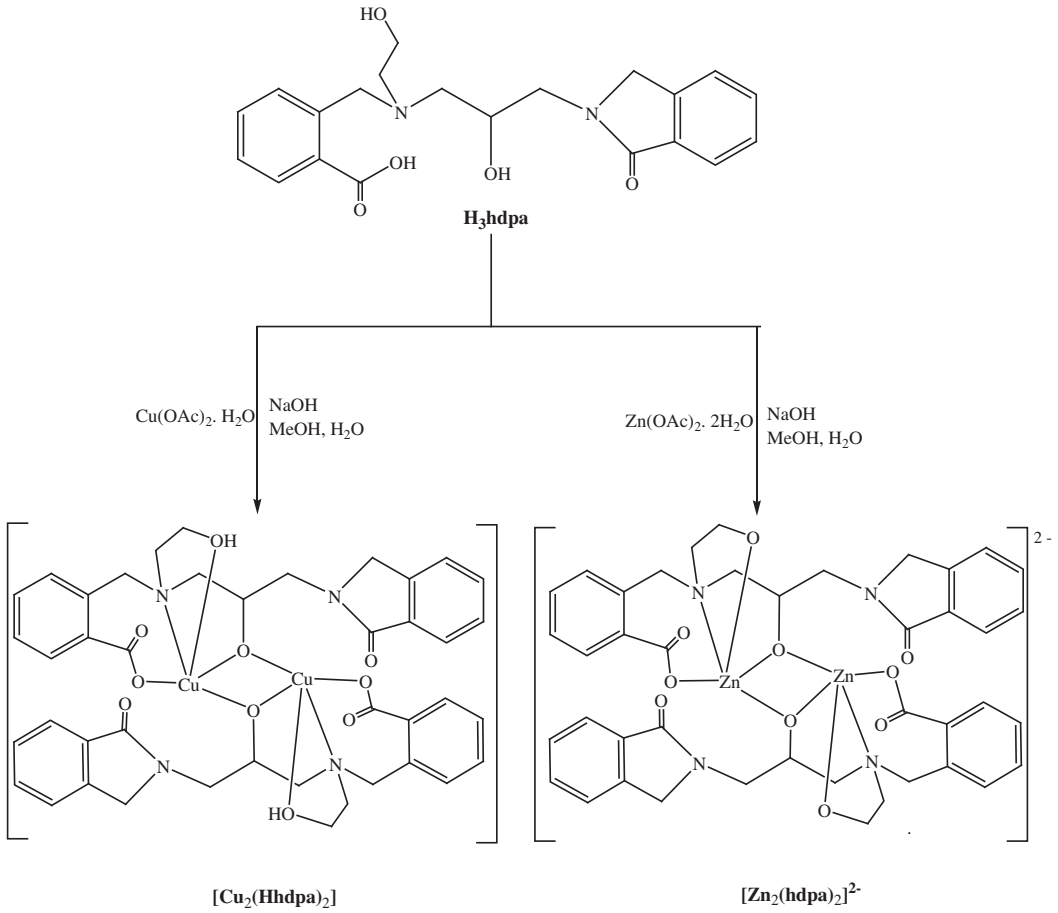

Scheme 2. Synthesis of complexes **1** and **2**.

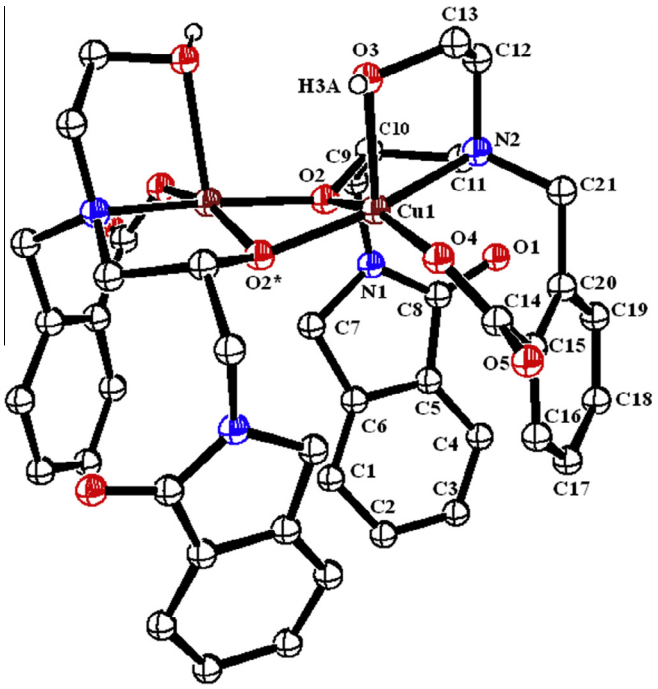

Fig. 2. Thermal ellipsoid (35%) drawing of the molecular structure of the complex $[Cu_2(Hhdpa)_2]\cdot 2CH_3OH\cdot 6H_2O$ (**1**) with the atom numbering scheme. Hydrogen atoms are omitted for clarity.

all possible isomers of the complex without any symmetry restrictions. The lowest energy isomer is reported here. The vibrational frequencies were analyzed to confirm the identity of the stationary point and it was found to be a minimum (without any negative frequency). A view of the optimized structure is shown in Fig. 3. Selected bond distances and bond angles are given in Table 3. The dianionic species $[Zn_2(hdpa)_2]^{2-}$ consists of two equivalent zinc(II) ions bridged by the central alkoxo oxygen atoms of the two ligands, forming a $Zn_2(OR)_2$ central core. According to the calculated optimized structure, each zinc center is pentacoordinated with two bridging alkoxo oxygens, one terminal alkoxo oxygen, one tertiary amine nitrogen and one benzoate oxygen atom of the ligand. The coordination geometry around the zinc centre is distorted trigonal bipyramid. The trigonality factor (τ) is 0.52; $\tau = 0$ for an ideal square pyramid and $\tau = 1$ for an ideal trigonal bipyramid [27]. The trigonal bipyramidal geometry around Zn(100) is defined by the O(75), O(79) and O(80) atoms at equatorial positions, and O(30) and N(92) atoms at axial positions. The equatorial bond lengths around the Zn(100) atom are in the range 1.981–2.074 Å. The Zn(100)–O(30) and Zn(100)–N(92) axial bond distances are 2.049 and 2.378 Å, respectively. The Zn(100)–N(92) axial bond distance is significantly longer, which is in agreement with the values reported in the literature [28]. The Zn–Zn separation in the dinuclear unit is 3.124 Å, which is comparable to those reported in the literature [29]. As observed in the single crystal X-ray structure of complex **1**, the DFT optimized structure of complex **2** also exhibits that the isoindol functionality at the half end of the ligand $hdpa^{3-}$ remains uncoordinated to any of the zinc(II) centers.

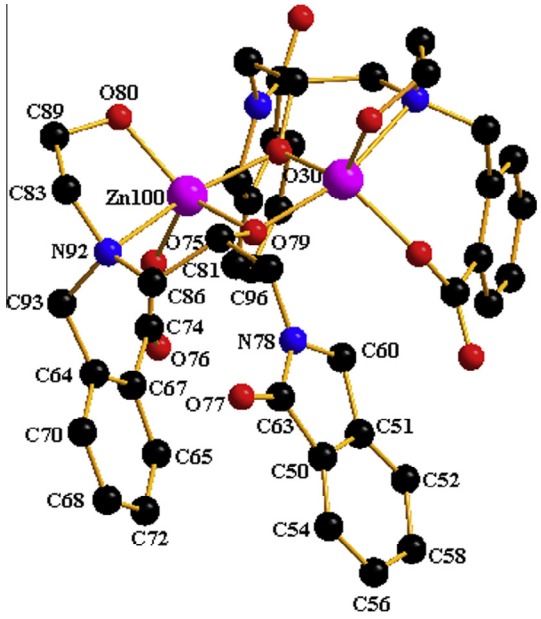

Fig. 3. DFT optimized molecular structure of the complex $Na_4[Zn_2(hdpa)_2](OAc)_2$ (**2**) with the atom numbering scheme. Hydrogen atoms are omitted for clarity.

3.4. Description of the NMR spectra of $Na_4[Zn_2(hdpa)_2](OAc)_2$ (**2**)

A combined approach of ^1H and ^{13}C NMR spectroscopic techniques also authenticated the identity of the dinuclear zinc(II) complex **2**. The ^1H NMR spectrum of complex **2** shows two sharp singlets at 2.88 and 4.59 ppm that correspond to a set of benzylic protons and a set of ethylenic protons of the isoindol ring, respectively. The spectrum also displays broad multiplets in the range 3.47–4.71 ppm, corresponding to the remaining ethylenic and propylenic protons, which suggest exchange on the NMR timescale with the water protons in the solvent. The spectrum contains a sharp singlet resonance peak at 1.80 ppm which can be assigned to the methyl protons of the uncoordinated acetate group. In addition, broad multiplets are observed in the range 7.48–7.94 ppm, indicating the presence of sixteen aromatic protons. The ^{13}C NMR spectrum of the complex **2** (Fig. S4 in the SI) displays a chemical shift at 177.17 ppm that corresponds to the benzoate carbon atom. The characteristic ^{13}C NMR signal at 167.68 ppm also confirms the presence of an uncoordinated acetate group in the complex. The methylene carbon and carbonyl carbon for the isoindol functionality are observed at 51.12 and 162.40 ppm, respectively. The aromatic carbons appear in the range 122.71–142.25 ppm. The carbon bearing the alkoxo oxygen appears at 68.10 ppm, whereas for the free H_3hdpa ligand it appears at 66.35 ppm.

Table 3
Selected bond lengths [Å] and angles [deg] in complex **2** calculated by DFT methods.

Bond lengths (Å)	
Zn(100)–O(80)	1.9805
Zn(100)–O(75)	2.0415
Zn(100)–O(30)	2.0493
Zn(100)–O(79)	2.0736
Zn(100)–N(92)	2.3782
Bond angles (°)	
O(80)–Zn(100)–O(75)	108.430
O(80)–Zn(100)–O(30)	105.890
O(80)–Zn(100)–O(79)	127.187
O(80)–Zn(100)–N(92)	82.949
O(75)–Zn(100)–O(30)	106.879
O(75)–Zn(100)–O(79)	119.467
O(75)–Zn(100)–N(92)	88.029
O(30)–Zn(100)–O(79)	81.217
O(30)–Zn(100)–N(92)	158.576
O(79)–Zn(100)–N(92)	78.005

3.5. FTIR and mass spectroscopic studies

We have examined the FTIR spectra of complexes **1** and **2** in order to draw useful conclusions for the correlations between the carboxylate stretching frequencies and their geometries [10d,30]. In the FTIR spectrum of complex **1**, two strong bands at 1587 and 1382 cm^{-1} are due to the asymmetric and symmetric stretching vibrations of the terminal benzoate group of the ligand, respectively. The difference of ~205 cm^{-1} between the asymmetric and symmetric stretching vibrations is attributed to terminal monodentate binding of the benzoate group. Similarly, in the FTIR spectrum of complex **2** (Fig. S5 in the SI), two strong bands at 1591 and 1340 cm^{-1} correspond to the asymmetric and symmetric stretching vibrations of the terminal benzoate functionality of the ligand, respectively. The difference of ~251 cm^{-1} between the asymmetric and symmetric stretching vibrations indicates a terminal monodentate binding of the benzoate functionality. The significantly high values of Δ ($\Delta = \nu_{as(COO-)} - \nu_{s(COO-)}$) for the terminal monodentate coordination has been observed in the literature [31,32]. Additionally, the FTIR spectrum of complex **2** displays asymmetric and symmetric carboxylate stretches at 1567 and 1399 cm^{-1} respectively, (Δ = 168 cm^{-1}) suggesting the presence of an ionic acetate group outside of the coordination sphere [33]. Further, the lack of a strong band at 540 cm^{-1} ($\pi(CO_2)$) indicates that the acetate group is not monodentate, confirming its presence as the counter anion. The FTIR spectra of complex **1** and **2** also exhibit a sharp band at ~1656 cm^{-1} assignable to the ν(C=O) vibration of the uncoordinated isoindol functionality.

In order to further characterize the complexes, methanolic solution of **1** was positive-ion electrosprayed and methanolic solution of **2** was negative-ion electrosprayed into a quadrupole ion-trap mass spectrometer and subjected to collision-induced dissociation to gain structural information. The mass spectrum of complex **1** (Fig. S6 in the SI) shows a signal at m/z = 914 that corresponds to the $\{[Cu_2(Hhdpa)_2]+Na\}^+$ species, confirming the dimetallic nature of complex **1** in solution. The mass spectrum of complex **2** (Fig. S7 in the SI) yields a signal at m/z = 1014 that corresponds to the $\{[Zn_2(hdpa)_2]\ (OAc)_2+3H\}^-$ species, confirming the dimetallic nature of complex **2** in solution. Therefore, the mass spectral analyses suggest that both dinuclear complexes are stable, even in solution.

3.6. Magnetic properties of $[Cu_2(Hhdpa)_2]\cdot 2CH_3OH\cdot 6H_2O$ (**1**)

The magnetic properties of the dinuclear copper(II) complex **1** was studied on a powder sample by variable temperature magnetic susceptibility measurements. The susceptibility data were collected in the temperature range 2–300 K in an applied field of 1 Tesla and are shown as a $\chi_M T$ versus T plot in Fig. 4. At room temperature, a $\chi_M T$ value of 0.65 $cm^3\ K\ mol^{-1}$ can be observed, which is slightly lower than the expected value of 0.75 $cm^3\ K\ mol^{-1}$ for two uncoupled spins with $S_1 = S_2 = ½$. On lowering the temperature to 20 K, a decrease of the $\chi_M T$ value can be observed, reaching a value of 0.05 $cm^3\ K\ mol^{-1}$. Further cooling leads to no significant decrease of the $\chi_M T$ value. This indicates an antiferromagnetic interaction between the two copper(II) ions. The magnetic data can be simulated satisfactorily by applying the isotropic exchange Hamilton operator: $\hat{H} = -2J\hat{S}_1\hat{S}_2$. The best simulation is obtained with J = −52.20 cm^{-1} and $g_1 = g_2$ = 2.041. A paramagnetic impurity of 11% with S = ½ has to be included to obtain a good simulation (blue line). In alkoxo bridged dinuclear copper(II) complexes with

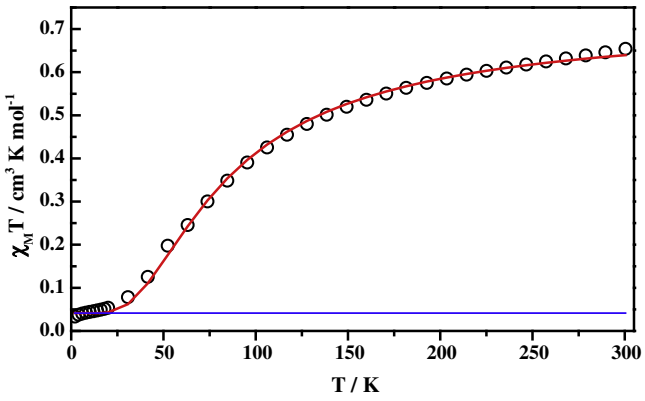

Fig. 4. Temperature dependence of $\chi_M T$ vs. T for the complex $[Cu_2(Hhdpa)_2]\cdot 2CH_3OH\cdot 6H_2O$ (**1**). The red solid line corresponds to the best fit obtained with the Hamilton described in the text. (Colour online.)

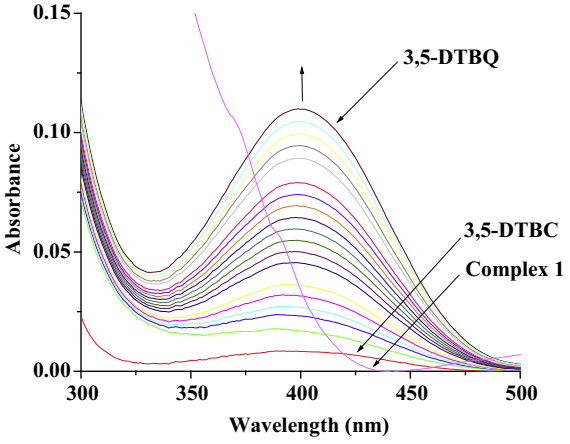

Fig. 5. UV–Vis spectra (300–500 nm) of (i) complex **1** (0.5×10^{-4} M) in methanol; (ii) 3,5-DTBC (0.5×10^{-2} M) in methanol; (iii) changes in UV–vis spectra of complex **1** (0.5×10^{-4} M) upon addition of 100-fold 3,5-DTBC in methanol observed after each 5 min interval.

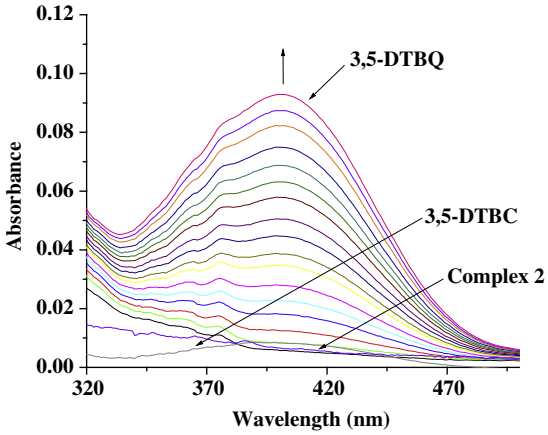

Fig. 6. UV–Vis spectra (320–500 nm) of (i) complex **2** (0.5×10^{-4} M) in methanol; (ii) 3,5-DTBC (0.5×10^{-2} M) in methanol; (iii) changes in UV–Vis spectra of complex **2** (0.5×10^{-4} M) upon addition of 100-fold 3,5-DTBC in methanol observed after each 5 min interval.

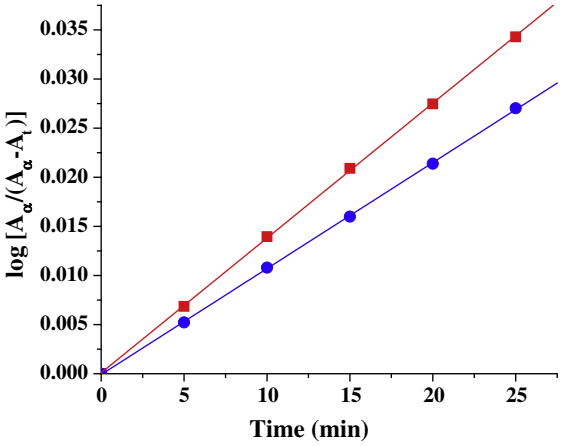

Fig. 7. Change of absorption maxima at 400 nm with time for complexes **1** (■) and **2** (●).

a $[Cu_2(\mu_2\text{-}O)_2]$ core, the magnetic coupling constant is influenced by several structural parameters, such as the Cu–O–Cu bridging angle (α), the hinge distortion of the $[Cu_2(\mu_2\text{-}O)_2]$ core (γ) and the out of plane shift of the carbon atoms of the alkoxo bridge (τ) [34,35]. A large bridging angle (α) favors strong antiferromagnetic interactions, while large γ and τ values lead to smaller antiferromagnetic or even ferromagnetic coupling constants. For complex **1**, with a bridging angle of 97.49°, a hinge distortion of 13.7° and an out of plane shift of the carbon atoms by 18°, a coupling constant J of -52.20 cm^{-1} can be found, which is in good agreement with the values given in the literature [36].

3.7. Catechol oxidase activity studies and kinetics

Catechol oxidase (CO), also known as *o*-diphenol oxidase, is a less well known member of the type-3 copper proteins [6b]. The official nomenclature is 1,2-benzenediol:oxygen oxidoreductase, indicating that dioxygen is the second substrate. CO catalyzes exclusively the oxidation of catechols (i.e., *o*-diphenols) to the corresponding *o*-quinones. The catalytic oxidation reaction of catechol, in particular, 3,5-di-tert-butylcatechol (3,5-DTBC), has been widely studied as a model reaction for catecholase activity. The substrate, 3,5-DTBC, with bulky substituents on the ring, has a low quinone-catechol reduction potential. This makes it easily oxidized to the corresponding *o*-quinone, 3,5-DTBQ, which is highly stable and exhibits a maximum absorption at 400 nm (ε = 1900 M^{-1} cm^{-1}) in methanol.

Prior to the detailed kinetic investigations, we examined the catecholase activity of complexes **1** and **2**, which showed catalytic oxidation activity towards the substrate 3,5-di-tert-butylcatechol. For this purpose 0.5×10^{-4} M solutions (in methanol) of these complexes were treated with a 0.5×10^{-2} M solution (~100 equiv.) of 3,5-DTBC at room temperature under aerobic conditions. The course of the reaction was followed by the UV–vis spectroscopic technique. After addition of the substrate (3,5-DTBC) to solutions of catalysts **1** and **2**, a gradual increase in the band that corresponds to 3,5-di-tert-butyl-1,2-benzoquinone (3,5-DTBQ) was observed at 400 nm, as displayed in the UV–Vis spectra (Figs. 5 and 6).

The kinetics of the oxidation of 3,5-DTBC were determined from the initial rate method by monitoring the increase of the quinone band at 400 nm as a function of time. The concentration of the substrate 3,5-DTBC was always kept at least 10 times larger than that of the catalysts to maintain the pseudo-first-order reaction conditions. The rate constant for a particular complex-substrate product was evaluated from the $\log[A_\alpha/(A_\alpha - A_t)]$ versus time plot (Fig. 7). The solutions of complexes **1** and **2** were treated with different concentrations of 3,5-DTBC under aerobic conditions to determine

the dependence of the rates on the substrate concentration and various kinetic parameters. At low concentrations of substrate, a first-order dependence on the substrate concentration was observed, but at higher concentrations, saturation kinetics were observed for both complexes. Applying the Michaelis–Menten approach of enzymatic kinetics we have been able to get the Lineweaver–Burk (double reciprocal) plot using the equation $1/V = (K_M/V_{max})\ (1/[S]) + 1/V_{max}$ as well as the values of the various kinetic parameters, V_{max}, K_M and K_{cat}, which are reported in Table 4. The observed rate versus substrate concentration plot and the Lineweaver–Burk plot for complexes **1** and **2** are shown in Figs. 8 and 9. The turnover rates (K_{cat}) for complexes **1** and **2** are 17.05 and 9.13 h^{-1}, respectively, which are comparable to some reported model complexes [37–42] but are considerably lower than those reported by others [7a,c,43–46], and much lower than that of the native enzyme catechol oxidase isolated from sweet potatoes (Ipomoea batatas) ($K_{cat} = 8.25 \times 10^6\ h^{-1}$) [47].

Control experiments have also been performed under similar experimental conditions to examine the catecholase activity of copper(II) acetate, copper(II) chloride, zinc(II) acetate and zinc(II) chloride. The representative UV–Vis spectra for copper(II) acetate and zinc(II) acetate, showing the changes upon addition of 100-fold 3,5-DTBC in methanol observed after each 5 min interval, are given in Figs. S8 and S9 (Supporting information). The spectra clearly show that the catalytic oxidation activity of copper(II) acetate and copper(II) chloride is significantly lower than that of dinuclear copper(II) complex **1**, which is further supported by their extremely low turnover rates (K_{cat} for copper(II) acetate = 6.59 h^{-1} and K_{cat} for copper(II) chloride = 4.34 h^{-1}). Similarly, from the UV–Vis spectra, it is clear that the catalytic oxidation activity of zinc(II) acetate and zinc(II) chloride is negligible compared to that of the dinuclear zinc(II) complex **2**, which is further supported by their insignificant turnover rates (K_{cat} for zinc(II) acetate = 3.19 h^{-1} and K_{cat} for zinc(II) chloride = 0.09 h^{-1}). These results indicate that for the effective catalytic oxidation of 3,5-di-tert-butylcatechol (3,5-DTBC) to 3,5-di-tert-butyl-1,2-benzoquinone (3,5-DTBQ) under aerobic conditions the activation of the metal centers by coordination of a suitable ligand is essential.

Zubieta et. al. reported that for maximum catecholase activity the optimum M–M separation is in the range 2.9–3.2 Å, owing to the requirement for a steric match between the substrate and complex [48]. Although, the M–M separation in our present complexes is in the range of 2.9–3.1 Å, their low catalytic activity may be attributed to the fact that the two coordinated benzoate and two uncoordinated isoindol functionalities are significantly tilted in the same direction, making steric constraints during the interaction of 3,5-DTBC with the metal centers. We have also performed kinetic experiments by varying the catalyst concentrations and found a first-order rate dependence on the catalyst concentrations (Fig. S10 in the SI) [49].

We have compared the catecholase activity of complexes **1** and **2** by rationalizing the data obtained from the Lineweaver–Burk plot and found that the catalytic activity of complex **1** is higher than that of complex **2**. The different catalytic activities of complexes **1** and **2** are most likely due to two reasons. Firstly, there are different metal ions present in the respective complexes. Secondly, there are the differences in the coordination geometry around the metal centers in complexes **1** and **2**. The square pyramidal geometry around each copper(II) center in complex **1** more

Table 4
Kinetic parameters for complexes **1** and **2**.

Complex	V_{max} (M min^{-1})	K_m (M)	K_{cat} (h^{-1})
1	1.421×10^{-5}	5.039×10^{-3}	17.05
2	7.61×10^{-6}	1.78×10^{-2}	9.13

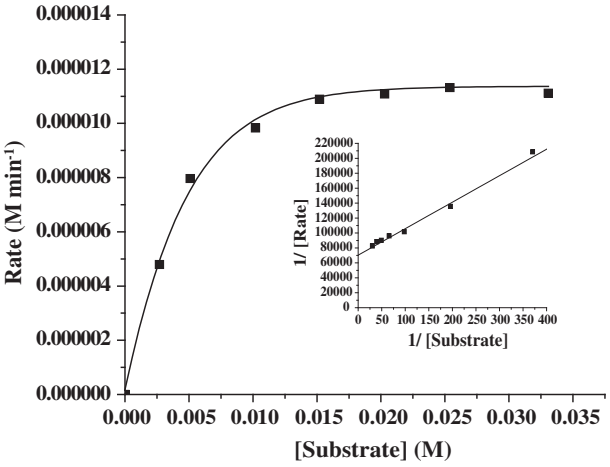

Fig. 8. Plot of rate vs. substrate concentration for complex **1**. Inset shows Lineweaver–Burk plot.

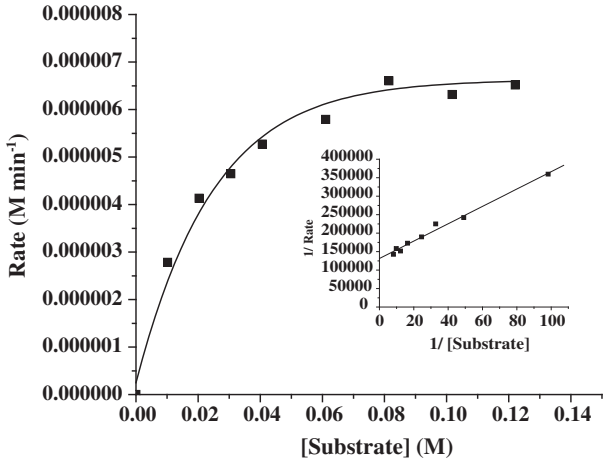

Fig. 9. Plot of rate vs. substrate concentration for complex **2**. Inset shows Lineweaver–Burk plot.

possibly facilitates the formation of complex-catecholate intermediates during the interaction with 3,5-DTBC compared to that in case of the trigonal bipyramidal geometry around each zinc(II) center in complex **2**.

3.8. DFT calculations

We have carried out DFT calculations to understand the binding process of 3,5-DTBC with complexes **1** and **2** during the catalytic oxidation reactions. The calculations have been performed on the neutral species $[Cu_2(Hhdpa)_2]$ (**1**) and the dianionic species $[Zn_2(hdpa)_2]^{2-}$ (**2**) and on the corresponding one-electron reduced analogues $\mathbf{1}^-$ and $\mathbf{2}^-$ at the UB3LYP and B3LYP levels respectively, using the Gaussian 03 software package. The structures of **1** and **2** proved to be the triplet ground state ($S = 1$) and the closed-shell singlet state ($S = 0$), respectively, with optimized structural parameters fully consistent with the crystallographic data. The one-electron-reduced species $\mathbf{1}^-$ and $\mathbf{2}^-$ display a doublet ($S = 1/2$) ground state. The calculated condensed Fukui function values f_k^+ at the metal centers of complexes **1** and **2** are given in Table 5. In complex **1**, the Fukui function values of the two copper centers are very close in magnitude and thereby it is presumed that 3,5-DTBC may bind with both the two copper centers with equal probability. Similarly, according to the values given in Table 5, it can be anticipated that

Table 5
Fukui functions of complexes **1** and **2**.

	1		**2**	
Atom	Cu	Cu	Zn	Zn
f_k^+	0.0357	0.0353	0.0186	0.0173

3,5-DTBC binds to two zinc centers with more or less equal probability because the Fukui function values f_k^+ of the two zinc centers are fairly close in magnitude. Again, the Fukui function values f_k^+ of the two zinc centers in complex **2** are significantly lower than those of the two copper centers in complex **1**, indicating the binding of 3,5-DTBC with complex **2** is weaker than that with complex **1**. This is also supported by the calculated turnover rates (K_{cat}) for complexes **1** and **2**, the values of which are 17.05 and 9.13 h^{-1}, respectively. Therefore, the DFT calculation results strongly suggest that during the catalytic oxidation reaction of 3,5-DTBC, its binding with the dinuclear complexes **1** and **2** occurs more possibly through the involvement of the two metal centers.

4. Conclusions

We have described the synthesis and characterization of a new dinuclear copper(II) complex (**1**) and a new dinuclear zinc(II) complex (**2**) of an isoindol functionality based dinucleating ligand. The X-ray structural and spectroscopic investigations confirmed the dimetallic nature of complexes **1** and **2**, both in the solid state as well as in solution. Complex **1** shows an antiferromagnetic interaction ($J = -52.20$ cm^{-1}) between the two copper centers, identified from variable temperature (2–300 K) magnetic susceptibility measurements. The complexes maintain a metal–metal separation falling in the range 2.9–3.1 Å which shows optimum cooperativity between the two metal centers for mimicking the structural and functional models to the active site of catechol oxidase. In a simulated metal–metal distance and NO_5 coordination environment, both the complexes show catecholase-like activity. Density Functional Theory (DFT) calculations strongly suggest that during the catalytic oxidation reaction of 3,5-DTBC, the binding of the substrate with the dinuclear metal complexes **1** and **2** occurs more possibly through the involvement of two metal centers. The present investigations will positively provide valuable insights into the biologically relevant coordination chemistry of copper and zinc.

Acknowledgements

The authors acknowledge the Department of Science and Technology (DST) (Grant No.: SR/FT/CS-067/2009), New Delhi for funding and financial support. The instrumental facilities provided by the DST-FIST and UGC-SAP program in the Department of Chemistry, University of Kalyani are greatly appreciated. A. P. thanks the University of Kalyani for providing a university research fellowship. The authors also acknowledge the Contingency Grant provided by the DST-PURSE program in the Department of Chemistry, University of Kalyani.

Appendix A. Supplementary data

CCDC 890493 contains the supplementary crystallographic data for **1**. These data can be obtained free of charge via http://www.ccdc.cam.ac.uk/conts/retrieving.html, or from the Cambridge Crystallographic Data Centre, 12 Union Road, Cambridge CB2 1EZ, UK; fax: +44 1223 336 033; or e-mail: deposit@ccdc.cam.ac.uk. Supplementary data associated with this article can be found, in the online version, at http://dx.doi.org/10.1016/j.poly.2013.09.034.

References

[1] (a) D.E. Fenton, H. Okawa, Perspectives on Bioinorganic Chemistry, vol. 2, JAI Press, London, UK, 1993. p. 81;
(b) K.D. Karlin, Science 261 (1993) 701.
[2] (a) R. Breslow, Acc. Chem. Res. 24 (1991) 317;
(b) A.J. Kirby, Angew. Chem., Int. Ed. Engl. 35 (1996) 707.
[3] (a) D.E. Wilcox, Chem. Rev. 96 (1996) 2435;
(b) N. Strater, W.N. Lipscomb, T. Klabunde, B. Krebs, Angew. Chem., Int. Ed. Engl. 35 (1996) 2024.
[4] (a) P.K. Nanda, V. Bertolasi, G. Aromi, D. Ray, Polyhedron 28 (2009) 987;
(b) J.E. Bol, W.L. Driessen, J. Reedijk, J. Chem. Soc., Chem. Commun. (1995) 1365;
(c) S. Torelli, C. Belle, I. Gautier-Luneau, J.L. Pierre, Inorg. Chem. 39 (2000) 3526;
(d) Y.C. Chou, S.F. Huang, R. Koner, G.H. Lee, Y. Wang, S. Mohanta, H. Wei, Inorg. Chem. 43 (2004) 2759.
[5] T. Klabunde, C. Eicken, J.C. Sacchettini, B. Krebs, Nat. Struct. Biol. 5 (1998) 1084.
[6] (a) A. Sanchez-Ferrer, J.N. Rodriguez-Lopez, F. Garcia-Canovas, F. Garciacarmona, Biochim. Biophys. Acta 1247 (1995) 1;
(b) E.I. Solomon, U.M. Sundaram, T.E. Machonkin, Chem. Rev. 96 (1996) 2563;
(c) C. Eicken, B. Krebs, J.C. Sacchettini, Curr. Opin. Struct. Biol. 9 (1999) 677;
(d) C. Gerdemann, C. Eicken, B. Krebs, Acc. Chem. Res. 35 (2002) 183.
[7] (a) A. Biswas, L.K. Das, M.G.B. Drew, C. Diaz, A. Ghosh, Inorg. Chem. 51 (2012) 10111;
(b) J. Mukherjee, R. Mukherjee, Inorg. Chim. Acta 337 (2002) 429;
(c) K.S. Banu, T. Chattopadhyay, A. Banerjee, S. Bhattacharya, E. Suresh, M. Nethaji, E. Zangrando, D. Das, Inorg. Chem. 47 (2008) 7083.
[8] A. Guha, T. Chattopadhyay, N.D. Paul, M. Mukherjee, S. Goswami, T.K. Mondal, E. Zangrando, D. Das, Inorg. Chem. 51 (2012) 8750.
[9] (a) M.E. Bodini, G. Copia, R. Robinson, D.T. Sawyer, Inorg. Chem. 22 (1983) 126;
(b) M. Ruf, B.C. Noll, M.D. Groner, G.T. Yee, C.G. Pierpont, Inorg. Chem. 36 (1997) 4860.
[10] (a) A. Patra, T.K. Sen, A. Ghorai, G.T. Musie, S.K. Mandal, U. Ghosh, M. Bera, Inorg. Chem. 52 (2013) 2880;
(b) A. Patra, T.K. Sen, R. Bhattacharyya, S.K. Mandal, M. Bera, RSC Adv. 2 (2012) 1774;
(c) M. Bera, A.B.S. Curtiss, G.T. Musie, D.R. Powell, Inorg. Chem. 51 (2012) 12093;
(d) M. Bera, G.T. Musie, D.R. Powell, Inorg. Chem. Commun. 13 (2010) 1029;
(e) M. Bera, G.T. Musie, D.R. Powell, Inorg. Chem. 48 (2009) 4625.
[11] (a) R.A. Joy, H. Arman, S. Xiang, G.T. Musie, Inorg. Chim. Acta 394 (2013) 220;
(b) C.H. Weng, S.C. Cheng, H.M. Wei, H.H. Wei, C.J. Lee, Inorg. Chim. Acta 359 (2006) 2029;
(c) A. Mukherjee, M.K. Saha, M. Nethaji, A.R. Chakravarty, New J. Chem. 29 (2005) 596;
(d) M. Kodera, N. Terasako, T. Kita, Y. Tachi, K. Kano, M. Yamazaki, M. Koikawa, T. Tokii, Inorg. Chem. 36 (1997) 3861.
[12] A.B.S. Curtiss, M. Bera, G.T. Musie, D.R. Powell, Dalton Trans. (2008) 2717.
[13] M. Kunishima, K. Hioki, T. Moriya, J. Morita, T. Ikuta, S. Tani, Angew. Chem., Int. Ed. 45 (2006) 1252;
(b) M. Pohmakotr, N. Yotapan, P. Tuchinda, C. Kuhakarn, V. Reutrakul, Tetrahedron 63 (2007) 4328;
(c) J.M. Concellon, E. Bardales, Org. Lett. 5 (2003) 4783.
[14] R.L. Carlin, Magnetochemistry, Springer–Verlag, New York, 1986.
[15] E. Bill, Max-Planck Institute for Bioinorganic Chemistry, Mülheim.
[16] (a) Data Collection: SMART Software Reference Manual, 1998. Bruker-AXS, 5465 E. Cheryl Parkway, Madison, WI 53711–5373, USA.;
(b) Data Reduction: SAINT Software Reference Manual, 1998. Bruker-AXS, 5465 E. Cheryl Parkway, Madison, WI 53711–5373, USA.
[17] G.M. Sheldrick, SADABS, Program for Multi-Scan Absorption Correction of Area Detector Data, University of Göttingen, Germany, 2002.
[18] (a) G.M. Sheldrick, SHELXTL; Version 6.10 Reference Manual. Bruker AXS, 5465 E. Cheryl Parkway, Madison, WI 53711–5373 USA, 2000.;
(b) International Tables for Crystallography, Vol C, Tables 6.1.1.4, 4.2.6.8 and 4.2.4.2, Kluwer. Boston, 1995.
[19] M.J. Frisch, G.W. Trucks, H.B. Schlegel, G.E. Scuseria, M.A. Robb, J.R. Cheeseman, J.A. Montgomery, T. Vreven, Jr., K.N. Kudin, J.C. Burant, J.M. Millam, S.S. Iyengar, J. Tomasi, V. Barone, B. Mennucci, M. Cossi, G. Scalmani, N. Rega, G.A. Petersson, H. Nakatsuji, M. Hada, M. Ehara, K. Toyota, R. Fukuda, J. Hasegawa, M. Ishida, T. Nakajima, Y. Honda, O. Kitao, H. Nakai, M. Klene, X. Li, J.E. Knox, H.P. Hratchian, J.B. Cross, C. Adamo, J. Jaramillo, R. Gomperts, R.E. Stratmann, O. Yazyev, A.J. Austin, R. Cammi, C. Pomelli, J.W. Ochterski, P.Y. Ayala, K. Morokuma, G.A. Voth, P. Salvador, J.J. Dannenberg, V.G. Zakrzewski, S. Dapprich, A.D. Daniels, M.C. Strain, O. Farkas, D.K. Malick, A.D. Rabuck, K. Raghavachari, J.B. Foresman, J.V. Ortiz, Q. Cui, A.G. Baboul, S. Clifford, J. Cioslowski, B.B. Stefanov, G. Liu, A. Liashenko, P. Piskorz, I. Komaromi, R.L. Martin, D.J. Fox, T. Keith, M.A. Al-Laham, C.Y. Peng, A. Nanayakkara, M. Challacombe, P.M.W. Gill, B. Johnson, W. Chen, M.W. Wong, C. Gonzalez, J.A. Pople, GAUSSIAN 03, Revision A.1; Gaussian, Inc., Pittsburgh, PA, 2003.
[20] (a) A.D. Becke, Phys. Rev. A 38 (1988) 3098;
(b) C. Lee, W. Yang, R.G. Parr, Phys. Rev. B 37 (1988) 785.

[21] (a) P.J. Hay, W.R. Wadt, J. Chem. Phys. 82 (1985) 299;
(b) W.R. Wadt, P.J. Hay, J. Chem. Phys. 82 (1985) 284;
(c) P.J. Hay, W.R. Wadt, J. Chem. Phys. 82 (1985) 270.
[22] W. Yang, W.J. Mortier, J. Am. Chem. Soc. 108 (1986) 5708.
[23] J.Y. Zhang, C.M. Liu, D.Q. Zhang, S. Gao, D.B. Zhuu, Inorg. Chim. Acta 360 (2007) 3553.
[24] D. Tran, B.W. Skelton, A.H. White, L.E. Laverman, P.C. Ford, Inorg. Chem. 37 (1998) 2505.
[25] S.A. Komaei, G.A. van Albada, I. Mutikainen, U. Turpeinen, J. Reedijk, Polyhedron 18 (1999) 1991.
[26] M. Koikawa, H. Yamashita, T. Tokii, Inorg. Chem. Commun. 6 (2003) 157.
[27] A.W. Addison, T.N. Rao, J. Reedijk, J. van Rijn, G.C. Verschoor, J. Chem. Soc., Dalton Trans. (1984) 1349.
[28] R.J. Pafford, T.B. Rauchfuss, Inorg. Chem. 37 (1998) 1974.
[29] (a) B.H. Ye, X.Y. Li, I.D. Williams, X.M. Chen, Inorg. Chem. 41 (2002) 6426;
(b) X.M. Chen, Y.X. Tong, T.C.W. Mak, Inorg. Chem. 33 (1994) 4586;
(c) A. Demsar, J. Kosmrlj, S. Petricek, J. Am. Chem. Soc. 124 (2002) 3951.
[30] G.B. Deacon, R.J. Phillips, Coord. Chem. Rev. 33 (1980) 227.
[31] V. Zelenak, I. Cisarova, P. Lewellyn, Inorg. Chem. Commun. 10 (2007) 27.
[32] V. Zelenak, M. Sabo, W. Massa, P. Llewellyn, Inorg. Chim. Acta 357 (2004) 2049.
[33] (a) V. Zelenak, Z. Vargova, K. Gyoryova, Spectrochim. Acta, Part A: Mol. Biomol. Spectrosc. 66 (2007) 262;
(b) D. Martini, M. Pellei, C. Pettinari, B.W. Skelton, A.H. White, Inorg. Chim. Acta 333 (2002) 72;
(c) A. Ross, J.H. Choi, T.M. Hunter, C. Pannecouque, S.A. Moggach, S. Parsons, E.D. Clercqc, P.J. Sadler, Dalton Trans. 41 (2012) 6408;
(d) B.H. Ye, F. Xue, G.Q. Xue, L.N. Ji, T.C.W. Mak, Polyhedron 18 (1999) 1785.
[34] E. Ruiz, P. Alemany, S. Alvarez, J. Cano, J. Am. Chem. Soc. 119 (1997) 1297.
[35] E. Ruiz, P. Alemany, S. Alvarez, J. Cano, Inorg. Chem. 36 (1997) 3683.
[36] K.R. Gruenwald, A.M. Kirillov, M. Haukka, J. Sanchizc, A.J.L. Pombeiro, Dalton Trans. (2009) 2109.
[37] J. Reim, R. Werner, W. Hasse, B. Krebs, Chem. Eur. J. 4 (1998) 289.
[38] (a) S. Majumder, S. Sarkar, S. Sasmal, E.C. Sanudo, S. Mohanta, Inorg. Chem. 50 (2011) 7540;
(b) S. Sarkar, S. Majumder, S. Sasmal, L. Carrella, E. Rentschler, S. Mohanta, Polyhedron 50 (2013) 270.
[39] A. Neves, L.M. Rossi, A.J. Bortoluzzi, A.S. Mangrich, W. Haase, R.J. Werner, J. Braz. Chem. Soc. 12 (2001) 747.
[40] V.K. Bhardwaj, N. Aliaga-Alcalde, M. Corbella, G. Hundal, Inorg. Chim. Acta 363 (2010) 97.
[41] K.S. Bharathi, S. Sreedaran, R.A. Ayswarya, A.K. Rahiman, K. Rajesh, V. Narayanan, J. Coord. Chem. 62 (2009) 600.
[42] D.M. Boghaei, M. Gharagozlou, M. Sayadi, J. Coord. Chem. 60 (2007) 2283.
[43] (a) A. Guha, K.S. Banu, A. Banerjee, T. Ghosh, S. Bhattacharya, E. Zangrando, D. Das, J. Mol. Catal. A 338 (2011) 51.
[44] F. Zippel, F. Ahlers, R. Werner, W. Haase, H.F. Nolting, B. Krebs, Inorg. Chem. 35 (1996) 3409.
[45] C.T. Yang, M. Vetrichelvan, X. Yang, B. Moubaraki, K.S. Murray, J.J. Vittal, Dalton Trans. (2004) 113.
[46] (a) X. Wang, J. Ding, J.J. Vittal, Inorg. Chim. Acta 359 (2006) 3481;
(b) K.S. Banu, T. Chattopadhyay, A. Banerjee, S. Bhattacharya, E. Zangrandoc, D. Das, J. Mol. Catal. A 310 (2009) 34.
[47] C. Eicken, F. Zippel, K. Buldt-Karentzopoulos, B. Krebs, FEBS Lett. 436 (1998) 293.
[48] K.D. Karlin, Y. Gultneh, T. Nicholson, J. Zubieta, Inorg. Chem. 24 (1985) 3725.
[49] J. Kaizer, G. Baráth, R. Csonka, G. Speier, L. Korecz, A. Rockenbauer, L. Párkañyi, J. Inorg. Biochem. 102 (2008) 773.